Tuning of Bloch modes, diffraction, and refraction by two-dimensional lattice reconfiguration

Peng Zhang,[1,2,*] Cibo Lou,[3] Sheng Liu,[1] Jianlin Zhao,[1] Jingjun Xu,[3] and Zhigang Chen[2,3]

[1]*Shaanxi Key Laboratory of Optical Information Technology, School of Science, Northwestern Polytechnical University, Xi'an 710072, China*

[2]*Department of Physics and Astronomy, San Francisco State University, San Francisco, California 94132, USA*

[3]*TEDA Applied Physics School, Nankai University, Tianjin 300457, China*

**Corresponding author: pengzhang.npu@gmail.com*

Received October 6, 2009; accepted February 12, 2010;
posted February 25, 2010 (Doc. ID 118233); published March 15, 2010

We demonstrate controlled excitation of Bloch modes and manipulation of diffraction and refraction in optically induced two-dimensional photonic lattices. Solely by adjusting the bias condition, the lattice structures can be reconfigured at ease, enabling the observation of transition between Bloch modes associated with different high-symmetry points of a photonic band, and interplay between normal and anomalous diffraction as well as positive and negative refraction under identical excitation condition. © 2010 Optical Society of America

OCIS codes: 050.1940, 080.1238, 190.5330.

Light propagating in optical periodic structures exhibits intriguing behavior that has no analog in homogeneous media [1]. For instance, linear anomalous diffraction and refraction has been observed in 1D waveguide arrays [2–5]. In the nonlinear regime, balance of discrete diffraction and nonlinearity leads to generation of discrete and gap solitons [6,7]. Subsequently, a host of fundamental phenomena were demonstrated in photonic lattices, including Bloch and Rabi oscillation [8,9], bandgap guidance through defects [10], and Anderson localization [11], to name just a few. Most of the experiments were done in optically induced lattices, where their structures can be reconfigured at ease by varying the intensity/pattern of the lattice-inducing beam (LIB).

Quite recently, we proposed that the anisotropic nonlinearity in a nonconventionally biased (NCB) photorefractive crystal could be used for self-trapping of novel spatial solitons, including discrete elliptical and "saddle" solitons [12–14]. In this Letter, we demonstrate theoretically and experimentally that, with lattice reconfiguration under the NCB condition, linear propagation of a 2D optical (probe) beam can be tailored. With the same LIB and without the need of changing the probe beam itself, we observe that the probe beam excites Bloch modes associated with different high-symmetry points, displays normal and anomalous diffraction, and exhibits positive and negative refraction simply by lattice reconfiguration. Our results could be relevant to similar phenomena in other reconfigurable discrete systems.

The steady-state propagation of a probe beam in a 2D photonic lattice under the NCB condition is governed by the following dimensionless equations [12]:

$$\left(\frac{\partial}{\partial z}-\frac{i}{2}\nabla^2\right)B(\vec{r})=i\left(\frac{\partial\varphi}{\partial x}\cos\theta_c+\frac{\partial\varphi}{\partial y}\sin\theta_c\right)B(\vec{r}), \tag{1a}$$

$$\nabla^2\varphi+\nabla\varphi\cdot\nabla\ln(1+I)=E_0\left[\frac{\partial\ln(1+I)}{\partial x}\cos\theta_e+\frac{\partial\ln(1+I)}{\partial y}\sin\theta_e\right], \tag{1b}$$

where $\nabla=\hat{x}(\partial/\partial x)+\hat{y}(\partial/\partial y)$, $B(\vec{r})$ is the amplitude of the probe beam, φ is the light-induced electrostatic potential, θ_e and θ_c represent the angle of the bias field E_0 and that of the crystalline c axis relative to the x axis, $I=V(x,y)+|B(\vec{r})|^2$ is the normalized total light intensity, $V(x,y)=\cos^2(\pi x/\Lambda)\cos^2(\pi y/\Lambda)$ corresponds to the intensity of the LIB with Λ being the spatial period, and the light-induced refractive index changes are determined by $(\partial\varphi/\partial x)\cos\theta_c+(\partial\varphi/\partial y)\sin\theta_c$. We use Eq. (1) for our modeling and use a setup similar to that in [13,14] for experiment. The periodic refractive index changes (index lattices) are induced with a gridlike intensity pattern (i.e., a periodically modulated LIB) in a biased crystal [$5\times10\times5(c)$ mm^3 SBN:60]. Typical induced lattice structures with the *same* LIB but under different bias conditions are presented in Fig. 1, where the top and bottom rows correspond to calculated index distributions and experimentally observed plane-wave guidance patterns of the induced lattices. For all results shown in Figs. 1(a)–1(d), the LIB has the same period of 17 μm, and the induced lattices approximately possess the same refractive index modulation of 1.5×10^{-4}, but the direction (relative to the c axis) and magnitude of the bias field are varied. Clearly, the induced lattice structure varies under different bias directions. Not only is the shape and orientation of individual lattice site changed, but also the locations of the index maxima can be shifted significantly with respect to those of the intensity maxima of the LIB, as driven by enhanced anisotropy and nonlocality [13]. The experimentally observed near-field pat-

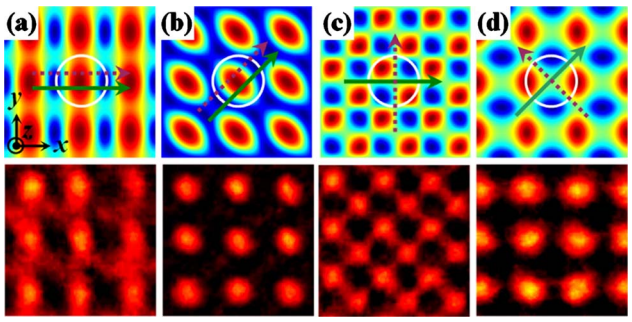

Fig. 1. (Color online) (top) Calculated refractive index distributions and (bottom) experimentally observed plane-wave guidance pattern of the optically induced lattices under different conditions. Solid and dashed arrows in the first row represent the directions of the c axis and bias field, and the white circle corresponds to an intensity spot of a square lattice-inducing beam. (a)–(d): $\theta_e=\theta_c=0$; $\theta_e=\theta_c=\pi/4$; $\theta_e=0$, $\theta_c=\pi/2$; $\theta_e=\pi/4$, $\theta_c=3\pi/4$. The corresponding bias fields are 2.4, 3.4, 8, and 3.2 kV/cm, respectively.

terns of the induced lattices are in good agreement with results from our theoretical calculation.

We now focus on the behavior of a probe beam propagating linearly through the above induced lattices. Take Figs. 1(c) and 1(d) as an example; the period and orientation of these two induced lattice are quite different. We found that the first Brillouin zone (BZ) of the lattice in Fig. 1(c) happens to be overlapping with the second BZ of the lattice in Fig. 1(d). Therefore the high-symmetry M_1 point in one setting [Fig. 1(d)] corresponds to the X_1 point in another setting [Fig. 1(c)], as also illustrated in the band diagrams in Figs. 2(a)–2(c). This enables the excitation of Bloch modes associated with different high-symmetry points [15] in the first band with same excitation scheme. Typical results are shown in Figs. 2(d)–2(g), where the Bloch modes are excited in these two lattices established under different NCB conditions. In our experiment, the probe beam is tilted at the same angle to excite the Bloch modes at M_1/X_1 point marked by a solid (green) dot in Figs. 2(a)–2(c). With both the probe beam and the LIB kept unchanged, transition between Bloch modes at M_1 [Figs. 2(d) and 2(e)] and X_1 [Figs. 2(f) and 2(g)] is realized by rotating the biased crystal 45° about the z axis. The measured intensity and phase (via interference) structures confirmed such a transition, in excellent agreement with calculated results.

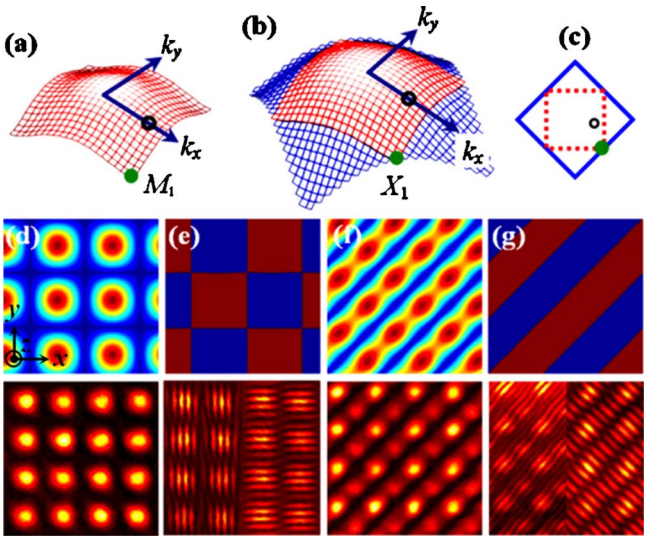

Fig. 2. (Color online) Demonstration of Bloch-mode transition by lattice reconfiguration. (a) and (b) illustrate the first-band diagram corresponding to lattices of Figs. 1(d) and 1(c), respectively; (c) shows the boundary of the first BZ for (a) and (b); (d)–(g) are (top) calculated and (bottom) experimentally observed [(d), (f)] intensity and [(e), (g)] phase structures of Bloch modes excited at the solid green spots marked in (a)–(c) for lattices illustrated [(d), (e)] in Fig. 1(d) and [(f), (g)] in Fig. 1(c).

Since beam diffraction in 2D lattices depends on the position of its Bloch momentum vector within the BZ, we next show the transition between normal and anomalous diffraction using the above overlapping BZs. The region of normal diffraction for one lattice [Fig. 1(c)] but of anomalous diffraction along k_x for other lattices [Figs. 1(a), 1(b), and 1(d)] can be identified (marked by a black circle in Fig. 2). By employing a tilted Gaussian beam (waist located before the front facet of the crystal) as probe whose transverse **k**-vector corresponds to the black circle in Fig. 2, we observe different 2D diffraction patterns coming from different lattices, as shown in Fig. 3. Clearly, the beam exhibits normal diffraction in both transverse directions in Fig. 3(c) but anomalous diffraction along k_x in Figs. 3(a), 3(b), and 3(d). Such anomalous diffraction has been demonstrated previously either by tuning the angle in 1D lattices [2] or tuning the nonlinearity in 2D lattices [15], but here the transition between *linear* normal and anomalous diffraction is realized with the *same* input tilt simply by reconfiguring the 2D photonic lattices.

Finally, we show that by lattice reconfiguration a probe beam can also excite Bloch modes from different bands, permitting the transition between normal (positive) and anomalous (negative) refraction [3]. An example is illustrated in Fig. 4, where the two-beam excitation technique [4] is employed to selectively excite Bloch modes. The angle between the two input beams is set to be twice of the Bragg angle, while the added input direction of the two interfering beams is tilted by a half Bragg angle. Under this condition, the

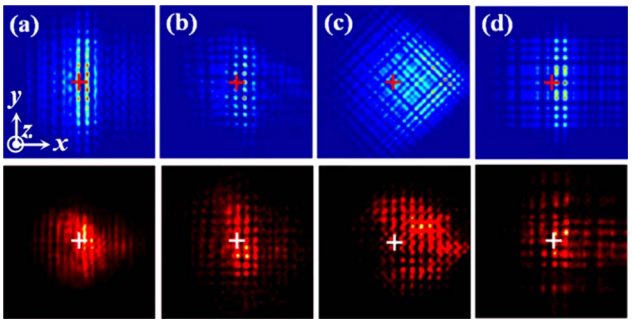

Fig. 3. (Color online) Demonstration of 2D normal and anomalous diffraction by lattice reconfiguration. (a)–(d) Numerical (top) and experimental (bottom) results of output diffraction patterns of the same probe beam [excitation position marked by the circles in **k**-space of Figs. 2(a)–2(c)] from the four lattices shown in Figs. 1(a)–1(d), respectively. The crosses indicate the center of the input beam.

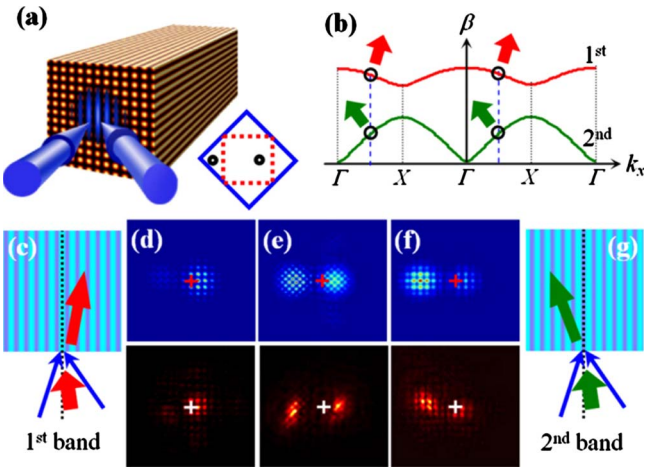

Fig. 4. (Color online) Demonstration of 2D positive and negative refraction by lattice reconfiguration. (a) Excitation scheme with locations in **k**-space of the two input beams marked by circles in inset. (b) Direction of refracted light (marked by arrows) at the first- and second-band diffraction curves. (c), (g) Illustration of light refraction from the first and second bands. (d)–(f) Numerical (top) and experimental (bottom) results of the output probe beam from lattices in Figs. 1(b)–1(d), respectively. The crosses indicate the center of the two beams at input.

k_x component of one of two beams is positioned inside the first BZ, but that of the other beam is outside [in lattices of Figs. 1(b) and 1(d)]. In addition, the interference maxima of the two beams are kept overlapping with the intensity maxima of the LIB. However, as seen in Fig. 1, reconfiguration of the lattices could result in a change from on-site to off-site excitation [e.g., from Fig. 1(b) to Fig. 1(d)]. This in turn leads to a change of excitation of Bloch modes from the first to the second band [Fig. 4(b)], and therefore a change of apparent refraction of the probe beam from anomalous [Figs. 4(c) and 4(d)] to normal [Figs. 4(f) and 4(g)]. Three cases are shown in Figs. 4(d)–4(f), corresponding to outputs from lattices of Figs. 1(b)–1(d), respectively. For all these cases, the input direction of the two beams (or the direction of total energy flow) is initially tilted toward the left, and it bends further to left in Figs. 4(f) and 4(g) owing to dominant excitation of the second-band Bloch modes by both beams in the periodic structure. However, it bends back to the right (anomalous refraction) in Figs. 4(c) and 4(d) owing to dominant excitation of the first-band Bloch modes [Fig. 4(b)]. From the direction of the energy flow depicted in Fig. 4(c), it can be seen that the anomalous refraction represents just a negative refraction of energy flow, similar to that observed in other periodic systems [16]. Since the input pattern from the two-beam interference does not perfectly match that of the first-band Bloch mode, a weak second-band excitation also occurs in Fig. 4(d) where the left spot does not disappear completely. For the lattice shown in Fig. 1(c), both input beams excite different first-band Bloch modes within the same first BZ owing to an increased size of BZ in this case, and thus the directions of the energy flow of the two beams cannot be reoriented to the same direction [Fig. 4(e)].

In summary, we have demonstrated controllable tuning of Bloch modes, diffraction, and refraction by sending a 2D probe beam into reconfigurable photonic lattices. Our results may have direct impact on the studies of wave dynamics in other reconfigurable periodic systems.

This work was supported by the Northwestern Polytechnical University (NPU) Foundation for Fundamental Research, the Doctorate Foundation of NPU, the 973 program (2007CB613203), 111 project, the National Natural Science Foundation of China (NSFC), Program for Changjiang Scholars and Innovative Research Team, National Science Foundation (NSF), and the Air Force Office of Scientific Research.

References

1. D. N. Christodoulides, F. Lederer, and Y. Silberberg, Nature **424**, 817 (2003).
2. H. S. Eisenberg, Y. S. Silberberg, R. Morandotti, and J. S. Aitchison, Phys. Rev. Lett. **85**, 1863 (2000).
3. T. Pertsch, T. Zentgraf, U. Peschel, A. Bräuer, and F. Lederer, Phys. Rev. Lett. **88**, 093901 (2002).
4. C. R. Rosberg, D. N. Neshev, A. A. Sukhorukov, Y. S. Kivshar, and W. Krolikowski, Opt. Lett. **30**, 2293 (2005).
5. R. Morandotti, H. S. Eisenberg, Y. Silberberg, M. Sorel, and J. S. Aitchison, Phys. Rev. Lett. **86**, 3296 (2001).
6. J. W. Fleischer, M. Segev, N. K. Efremidis, and D. N. Christodoulides, Nature **422**, 147 (2003).
7. H. Martin, E. D. Eugenieva, Z. Chen, and D. N. Christodoulides, Phys. Rev. Lett. **92**, 123902 (2004).
8. H. Trompeter, W. Krolikowski, D. N. Neshev, A. S. Desyatnikov, A. A. Sukhorukov, Y. S. Kivshar, T. Pertsch, U. Peschel, and F. Lederer, Phys. Rev. Lett. **96**, 053903 (2006).
9. K. Shandarova, C. E. Rüter, D. Kip, K. G. Makris, D. N. Christodoulides, O. Peleg, and M. Segev, Phys. Rev. Lett. **102**, 123905 (2009).
10. I. Makasyuk, Z. Chen, and J. Yang, Phys. Rev. Lett. **96**, 223903 (2006).
11. T. Schwartz, G. Bartal, S. Fishman, and M. Segev, Nature **446**, 52 (2007).
12. P. Zhang, J. Zhao, C. Lou, X. Tan, Y. Gao, Q. Liu, D. Yang, J. Xu, and Z. Chen, Opt. Express **15**, 536 (2007).
13. P. Zhang, J. Zhao, F. Xiao, C. Lou, J. Xu, and Z. Chen, Opt. Express **16**, 3865 (2008).
14. Y. Hu, C. Lou, P. Zhang, J. Xu, J. Yang, and Z. Chen, Opt. Lett. **34**, 3259 (2009).
15. D. Träger, R. Fischer, D. N. Neshev, A. A. Sukhorukov, C. Denz, W. Królikowski, and Y. S. Kivshar, Opt. Express **14**, 1913 (2006).
16. C. Luo, S. G. Johnson, J. D. Joannopoulos, and J. B. Pendry, Phys. Rev. B **65**, 201104 (2002).